Article

Synthesis, Structures and Properties of Molecular Conductors Based on Bis-Fused Donors Composed of (Thio)Pyran-4-ylidene-1,3-dithiole and Tetraselenafulvalene

Ken-ichi Ishidzu, Minoru Ashizawa, Masaki Watanabe, Takashi Shirahata * and Yohji Misaki *

Department of Applied Chemistry, Graduate School of Science and Engineering, Ehime University, 3 Bunkyo-cho, Matsuyama 790-8577, Japan

* Authors to whom correspondence should be addressed; E-Mails: misaki.yohji.mx@ehime-u.ac.jp (Y.M.); shirataha.takashi.mj@ehime-u.ac.jp (T.S.); Tel.: +81-89-927-9920; Fax: +81-89-927-9920.
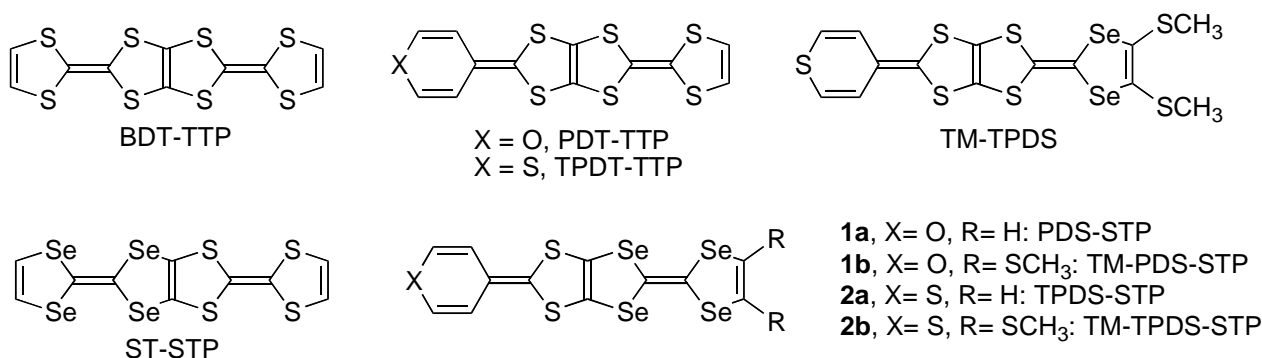
Abstract: Bis-fused donors composed of (thio)pyran-4-ylidene-1,3-dithiole and tetraselenafulvalene (**1a**, **2a**) and their bis(methylthio) derivatives (**1b**, **2b**) were synthesized. Cyclic voltamograms of all the donors consisted of four pairs of one-electron redox waves, and it was suggested that a positive charge of $1^{+\bullet}$ and $2^{+\bullet}$ distributed mainly on the (thio)pyran-4-ylidene-1,3-dithiole moiety. X-ray structure analysis revealed that $(\mathbf{1b})PF_6(C_6H_5Cl)_{0.5}$ and $(\mathbf{2b})PF_6(C_6H_5Cl)$ formed one-dimensional conducting stacks in which the donors were dimerized or tetramerized. In those salts, *intramolecular* charge disproportionation of the donors was suggested by X-ray structure analysis and density functional theory (DFT) calculation with UB3LYP/6-31G(d) basis function. A tight-binding band calculation suggested that these materials were band insulators. All the donors gave highly conducting TCNQ (7,7,8,8-tetracyanoquinodimethane) complexes and I_3^- salts ($\sigma_{rt} = 0.3$–19 S cm^{-1} on a compressed pellet) with very low activation energies of 0.017–0.040 eV, while single crystals of $(\mathbf{1b})PF_6(C_6H_5Cl)_{0.5}$ and $(\mathbf{2b})PF_6(C_6H_5Cl)$ exhibited semiconductive behavior with large activation energies ($E_a = 0.16$–0.22 eV).

Keywords: molecular conductor; tetrathiapentalene; pyran; thiopyran; tetraselenafulvalene; cyclic voltammetry; X-ray structure analysis; band calculation; electrical conductivity; *intramolecular* charge disproportionation

1. Introduction

In the development of molecular metals, a bis-fused TTF, 2,5-bis(1,3-dithiol-2-ylidene)-1,3,4,6-tetrathiapentalene (BDT-TTP or simply TTP) and its derivatives have played an important role [1–3]. They have actually produced a large number of molecular conductors exhibiting metallic behavior down to liquid helium temperature. Stable metallic behavior of BDT-TTP conductors is due to effective side-by-side interaction through sulfur atoms in the BDT-TTP framework, as well as reduced on-site Coloumb repulsion in the dicationic state [2,3]. Analogous TTP donor containing pyran-4-ylidene or thiopyran-4-ylidene donors, PDT-TTP and TPDT-TTP, where PDT-TTP and TPDT-TTP are 2-(1,3-dithiol-2-ylidene)-5-(pyran-4-ylidene)-1,3,4,6-tetrathiapentalene and 2-(1,3-dithiol-2-ylidene)-5-(thiopyran-4-ylidene)-1,3,4,6-tetrathiapentalene, respectively, are of significant interest. Thus, they are promising π-electron frameworks to explore three-dimensional (3D) conductors, because the chalcogen atom in the (thio)pyran ring could play a role for realizing considerable interaction along the donor long axis. We have synthesized a number of (T)PDT-TTP derivatives and their selenium analogues, and have investigated structures and properties of their conducting materials [4–7]. Among them, (TM-TPDS)$_2$AsF$_6$, where TM-TPDS is 2-[4,5-bis(methlylthio)-1,3-diselenol-2-ylidene]-5-(thiopyran-4-ylidene)-1,3,4,6-tetrathiapentalene gave 3D donor array [6], which is designated as a "windmill" arrangement, although the band structure was still quasi-1D owing to smaller "side-to-edge" interaction. In this connection, exchange of sulfur atoms in the central tetrathiapentalene moiety with selenium atoms is a promising strategy to increase 3D character in the conducting materials. No tetraselenapentalene-type donor has been synthesized so far because of synthetic difficulty. We have recently reported the synthesis of diselenadithiapentalene (STP) donor, 2-(1,3-diselenol-2-ylidene)-5-(1,3-dithio-2-ylidene)-1,3-deselena-4,6-dithiapentalene (ST-STP) [8,9]. In this paper, we report herein the synthesis and properties of new STP donors containing a series of chalcogenopyran-4-ylidene moiety, 2-(1,3-diselenol-2-ylidene)-5-(pyran-4-ylidene)-1,3-deselena-4,6-dithiapentalene (PDS-STP, **1a**), 2-(1,3-diselenol-2-ylidene)-5-(thiopyran-4-ylidene)-1,3-deselena-4,6-dithiapentalene (TPDS-STP, **2a**), and their bis(methylthio) derivatives (TM-PDS-STP **1b** and TM-TPDS-STP **2b**) (Figure 1). Structures and electrical properties of conducting materials based on these STP donors are also reported.

Figure 1. Molecular structures of BDT-TTP derivatives and their analogues.

BDT-TTP

X = O, PDT-TTP
X = S, TPDT-TTP

TM-TPDS

ST-STP

1a, X= O, R= H: PDS-STP
1b, X= O, R= SCH$_3$: TM-PDS-STP
2a, X= S, R= H: TPDS-STP
**2b**, X= S, R= SCH$_3$: TM-TPDS-STP

2. Results and Discussion

2.1. Synthesis

The new donors were synthesized according to Scheme 1. The reaction of 1,3-dithiole-2-thione fused with TSF (**3**) and tetrahydropyran-4-one (**4**) or tetrahydrothiopyran-4-one (**5**) in the presence of triethyl phosphite in refluxing toluene gave tetrahydro analogues of **1** and **2** (**6**,**7**) in 30–56% yields. Dehydrogenation of **6** and **7** with a slight excess (2.8 equiv. mol) of 2,3-dichloro-5,6-dicyano-*p*-benzoquinone (DDQ) in refluxing xylene afforded the target molecules **1** and **2** in 51–76% yields. The newly synthesized STP donors were obtained as stable ocher powder.

Scheme 1. Synthesis of **1** and **2**.
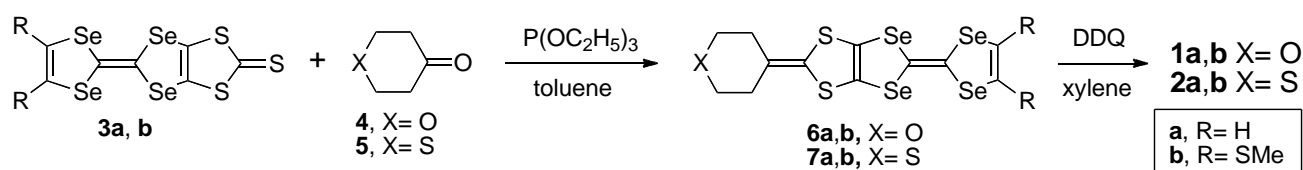

2.2. Electrochemical Properties

Electrochemical properties of new donors were investigated by cyclic voltammetry. Their redox potentials are summarized in Table 1. Cyclic voltamograms of all the new donors consisted of four pairs of one-electron redox waves. The first redox potentials (E_1) of **1** and **2** did not depend on the substituent on the TSF moiety, while the E_1 values varied on the chalcogen atom in the chalcogenopyran-2-ylidene moiety. In addition, the values of **1a** and **1b** were lower by 0.05–0.06 V than that of ST-STP (0.00 V). These results indicated that a positive charge formed by the first oxidation distributed on the 2-(chalcogenopyran-4-ylidene)-1,3-dithiole moiety mainly, and TSF moiety preferably acted as a selenium-based substituent. The second redox potential of **1a** was higher than that of **1b**, suggesting that the TSF moiety contributed to the second oxidation. These results suggested that intramolecular charge disproportionantion might occur in the conducting solids of **1** and **2**.

Table 1. Redox potentials of **1** and **2** (V *vs.* Fc/Fc$^+$ in benzonitrile containing 0.1 M Bu$_4$NPF$_6$).

Donor	E_1	E_2	E_3	E_4	$\Delta E \, (= E_2 - E_1)$
PDS-STP **1a**	−0.06	+0.26	+0.45	+0.67	0.32
TM-PDS-STP **1b**	−0.05	+0.30	+0.47	+0.67	0.35
TPDS-STP **2a**	−0.10	+0.22	+0.52	+0.72	0.32
TM-TPDS-STP **2b**	−0.09	+0.23	+0.53	+0.73	0.32
ST-STP	0.00	+0.30	+0.56	+0.74	0.30

The theoretical calculations of **1a** and **2a** were carried out using a density functional theory (DFT) B3LYP method with the 6-31G(d) basis set. Figure 2 shows the HOMOs of **1a** and **2a**. They distribute mainly to the chalcogenopyran-2-ylidene moiety and it is consistent with their redox property.

Figure 2. The HOMO of **1a** (left) and **2a** (right). The energy levels are −4.50 eV for **1a** and −4.52 eV for **2a**.
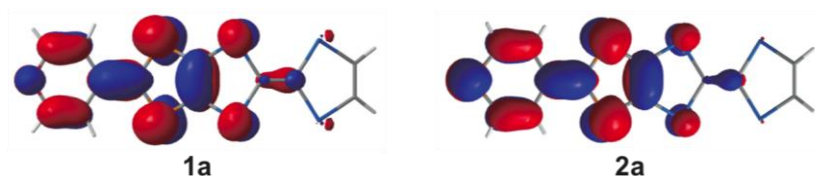
2.3. Molecular and Crystal Structures of a Neutral Molecule TM-PDS-STP (1b)

Single crystals of TM-PDS-STP (**1b**) were obtained by slow evaporation of the **1b** solution containing carbon disulfide. Figure 3 shows ORTEP drawings of TM-PDS-STP. The molecule is almost planar except for the carbon atoms in methylthio groups, which are projected over inclined upper direction. As shown in Figure 4, the molecules formed pseudo stack along the *a*-axis and are arranged in a so-called θ-type fashion. The interplanar distance along the pseudo stack is 3.54 Å. There is short Se··Se contact (3.624(1) Å) shorter than sum of van der Waals radii (Se··Se = 3.80 Å) [10].

Figure 3. ORTEP drawings of TM-PDS-STP. **(a)** Top view and **(b)** side view. Displacement ellipsoids are drawn at the 50% probability level.
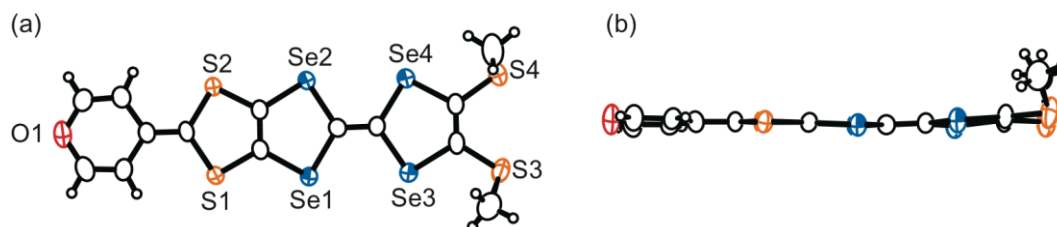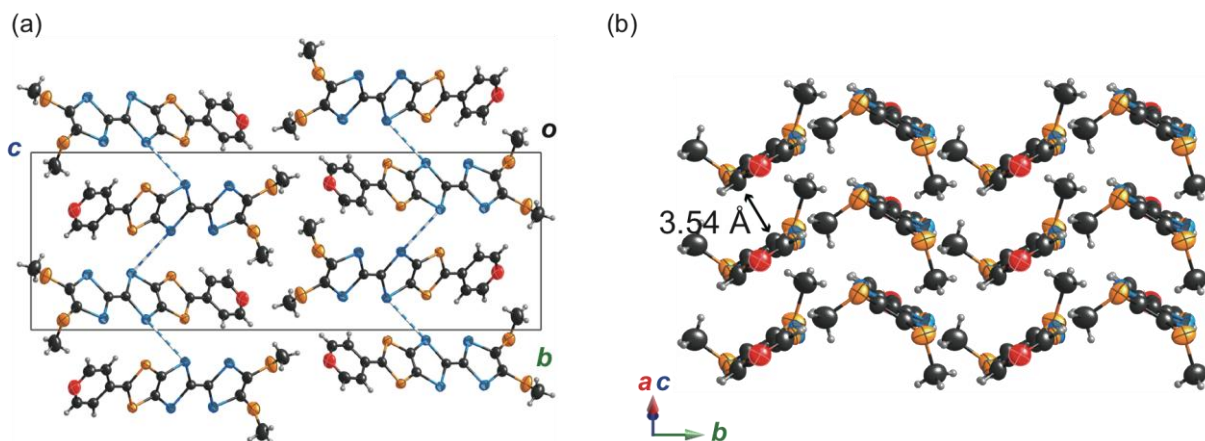

Figure 4. (a) Crystal structure of TM-PDS-STP viewed along the *a*-axis. Blue broken lines represent short Se··Se contacts shorter than sum of van der Waals radii; **(b)** Molecular arrangement of TM-PDS-STP viewed along the molecular long axis.

2.4. Preparation, Crystal and Band Structures of Radical Cation Salts

Radical cation salts of TM-PDS-STP (**1b**) and TM-TPDS-STP (**2b**) were grown by an electrocrystallization technique at a controlled current method [11] from 0.2 to 1.0 μA in the presence of the corresponding tetra-*n*-butylammonium salts as the supporting electrolyte in chlorobenzene (C_6H_5Cl) containing 5% ethanol at 35 °C. Crystallographic data for (TM-PDS-STP)PF_6(C_6H_5Cl)$_{0.5}$ and (TM-TPDS-STP)PF_6(C_6H_5Cl) are summarized in Table 3 (Experimental section). All the salts crystallize in triclinic system, space group $P\overline{1}$.

2.4.1. (TM-PDS-STP)PF_6(PhCl)$_{0.5}$

One donor molecule and anion were crystallographically independent, and were located on a general position. The PF_6^- anion showed disorder based on uni-axial rotation. The chlorobenzene was crystallographically unique and its chlorine atoms showed disorder at two positions. Moreover, the center of inversion exists in the benzene ring of the chlorobenzene, therefore, extreme disorder was observed. Figure 5 shows the ORTEP drawings of TM-PDS-STP molecule in (TM-PDS-STP)PF_6(C_6H_5Cl)$_{0.5}$. The donor molecule was almost planar; the deviations from the least-square plane are less than 0.45(2) Å except for the hydrogen atoms. The largest deviation (0.45(2) Å) is observed at the C14 position of the methylthio group. Both the methylthio groups were located the molecular plane, and projected outside of the molecular long axis in the plane composed of the donor skeleton. The crystal structure of (TM-PDS-STP)PF_6(C_6H_5Cl)$_{0.5}$ is shown in Figure 6. The molecules formed a face-to-face stack along the *a*-axis. The side-by-side interstack interactions were inhibited by the anions and disordered solvent molecules, which were located in the cavity formed by the donor molecules with large methylthio groups.

Figure 5. ORTEP drawings of TM-PDS-STP molecule in (TM-PDS-STP)PF_6(C_6H_5Cl)$_{0.5}$. (**a**) Top view and (**b**) side view. Displacement ellipsoids are drawn at the 50% probability level.
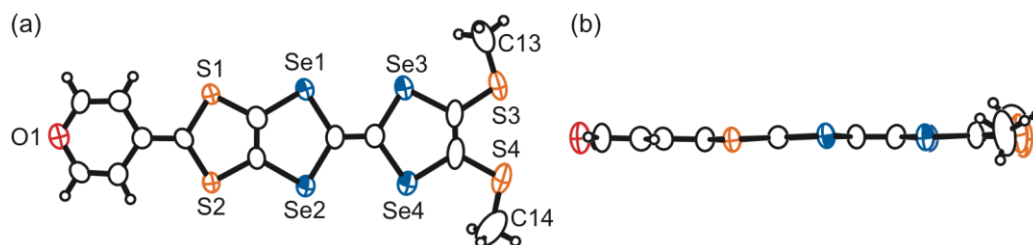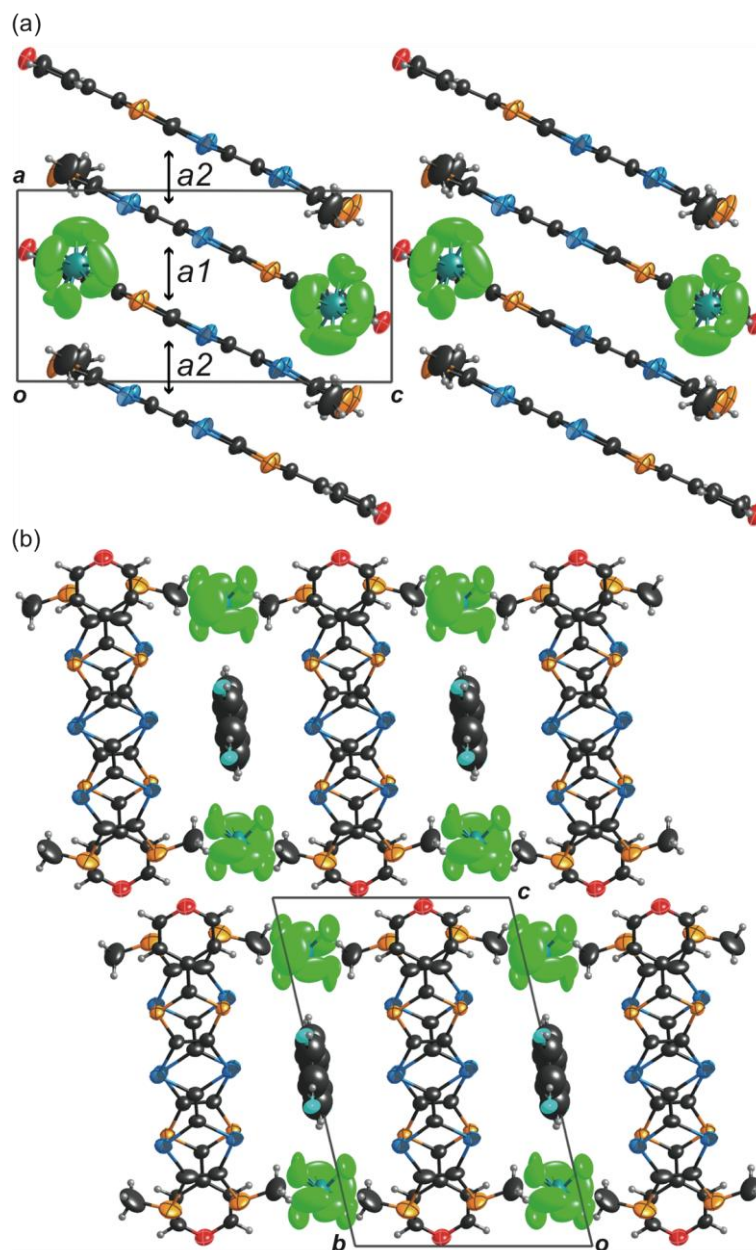
Figure 6. (a) Crystal structure of (TM-PDS-STP)PF$_6$(C$_6$H$_5$Cl)$_{0.5}$ viewed along the *b*-axis. The solvent molecules are omitted for clarity. **(b)** Crystal structure of (TM-PDS-STP)PF$_6$(C$_6$H$_5$Cl)$_{0.5}$ viewed along the *a*-axis.

The donors are dimerized in the stack, and were overlapped in a head-to-tail manner with interplanar distances of 3.54 Å for *a1* and 3.55 Å for *a2*, respectively. The slip distance along the molecular long axis for *a1* (1.18 Å) is smaller than that for *a2* (4.72 Å) as shown in Figure 7. Extended Hückel method is usually used for the calculation of the overlap integrals. This method does not contain Coulomb terms, that is, it is unsuitable when the calculation is carried out for the present charged species. The unrestricted DFT method using B3LYP functional with 6-31G(d) basis set was used for the charged donor (TM-PDS-STP)$^{•+}$ and the frontier molecular orbitals were summarized in Supplementary Materials (Figure S1). The SOMO of (TM-PDS-STP)$^{•+}$ distributes mainly to the TSF skeleton, while the HOMO-1 is dominantly localized on the (pyran-4-ylidene)-1,3-dithiole unit. The

energy level of the SOMO (−7.66 eV) is lower than that of the HOMO-1 (−7.46 eV), suggesting that the utilization of the HOMO-1 could be favorable for the calculation of overlap integrals of this salt. There is a difference in the bond length of C=C bond, which connects pyran ring and 1,3-dithiole ring, between the neutral state of TM-PDS-STP (1.35(1) Å) and the cation radical state of TM-PDS-STP (1.40(2) Å). In contrast, the bond length of the central C=C in TSF moiety is almost the same between neutral (1.34(1) Å) and cation radical (1.33(1) Å) state. These results indicate the distribution of positive charge on the (pyran-4-ylidene)-1,3-dithiole unit. Therefore, the overlap integrals were calculated by considering the HOMO-1 of the DFT calculation. The overlap integrals *a1* and *a2* are 16.0 and 7.3 $\times 10^{-3}$ and the donors are electronically dimerized along the stacking direction (Figure 8). Although the side-by-side interaction was prohibited owing to the presence of the anion and the solvent, the values of the overlap integrals *p1*, *p2*, and *p3* along the molecular long axis showed considerable magnitude due to the interactions among pyran units and thiomethyl groups. A tight-binding band calculation suggested that the salt is a band insulator.

Figure 7. Molecular overlap modes for *a1* and *a2* of (TM-PDS-STP)PF$_6$(C$_6$H$_5$Cl)$_{0.5}$. The atoms and bonds of the depth molecules are faded out.
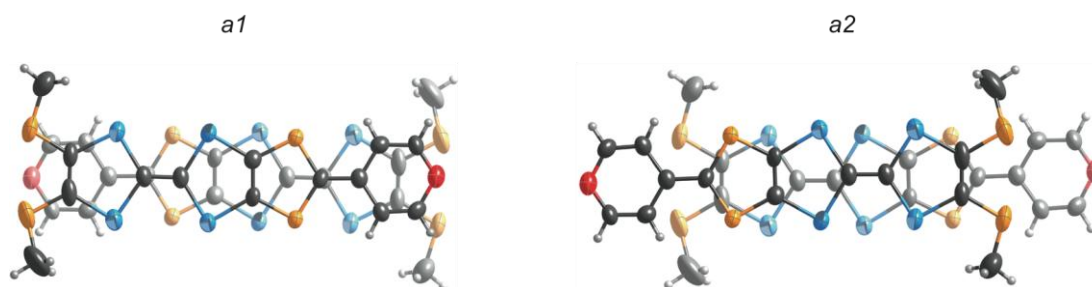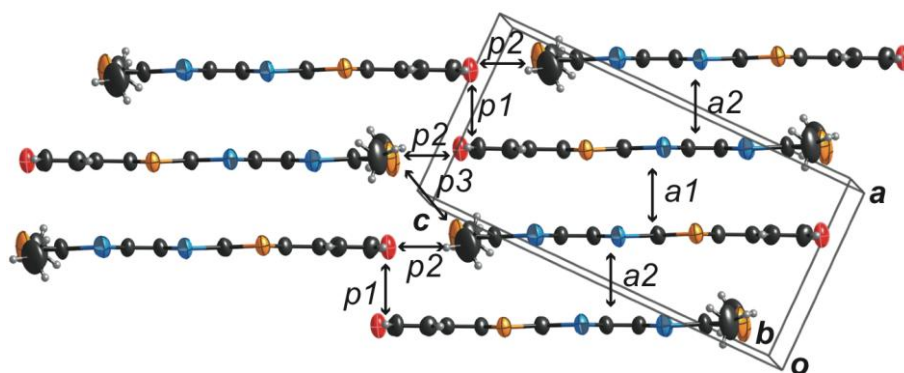

Figure 8. Donor sheet structure of (TM-PDS-STP)PF$_6$(C$_6$H$_5$Cl)$_{0.5}$ viewed along the molecular short axis. The calculated intermolecular overlaps between HOMO-1s ($\times 10^{-3}$) are *a1* = 16.0, *a2* = 7.3, *p1* = 1.1, *p2* = −2.2, and *p3* = 0.62.

2.4.2. (TM-TPDS-STP)PF$_6$(PhCl)

Two donor molecules, PF$_6^-$ anions, and chlorobenzene molecules were crystallographically independent, respectively, and the ratio of the donor, the anion, and the solvent is 1:1:1. One chlorobenzene molecule showed disorder and its chlorine atoms distribute to three positions with 1/3 of the occupancy. Figure 9 shows the ORTEP drawings of Molecule A and Molecule B in (TM-TPDS-

STP)PF$_6$(C$_6$H$_5$Cl). The molecular structure of Molecule A was almost planar. By contrast, the terminal 1,3-diselenole ring of Molecule B bent with dihedral angle of 9.7(3) °. Although the methyl groups of TM-PDS-STP were located on the molecular plane in (TM-PDS-STP)PF$_6$(C$_6$H$_5$Cl)$_{0.5}$, those of TM-TPDS-STP in (TM-TPDS-STP)PF$_6$(C$_6$H$_5$Cl) deviated from a least-square plane of donor π system; these deviations are 1.28(1) Å for C13, 0.50(1) Å for C14, 1.93(1) Å for C27, and 2.05(1) Å for C28.

Figure 9. ORTEP drawings of **(a, b)** Molecule A and **(c, d)** Molecule B of TM-TPDS-STP in (TM-TPDS-STP)PF$_6$(C$_6$H$_5$Cl) (top view and side view). Displacement ellipsoids are drawn at the 50% probability level.
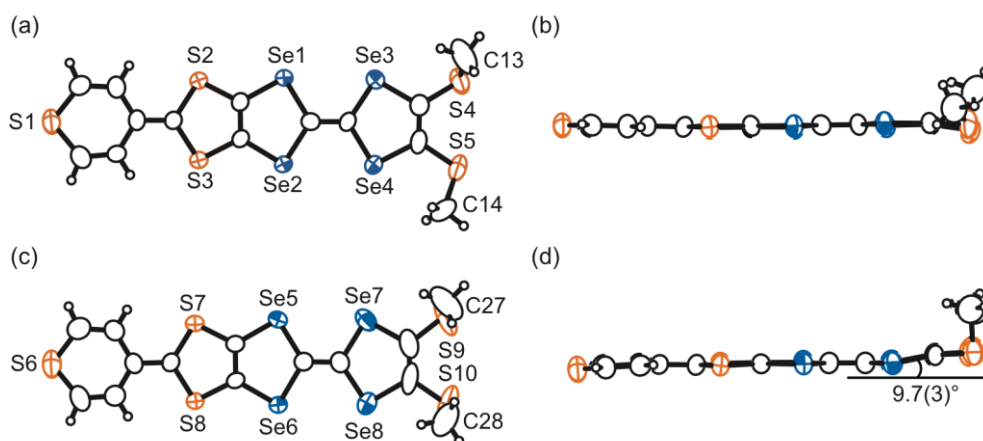
The crystal structure of (TM-TPDS-STP)PF$_6$(C$_6$H$_5$Cl) is shown in Figure 10. Molecule A and B formed a face-to-face stack with an -A-A-B-B-type four-fold periodicity along the *b–a* axis, indicating the presence of three intrastack overlaps *p1*, *p2*, and *p3* (Figure 11). The anions and chlorobenzene molecules were located between the donor molecules along the molecular short axis of TM-TPDS-STP, and they prevented side-by-side interaction between the donor molecules. The donor molecules A and B in this salt stacked in a head-to-tail manner with the interplanar distances 3.52 Å and 3.50 Å for the intermolecular interactions A-A (*p1*) and B-B (*p3*), and in a head-to-head manner with the interplanar distance 3.56 Å for A-B (*p2*) as shown in Figure 11. The slip distances of *p1*, *p2*, and *p3* are 4.59, 1.75, and 1.95 Å, respectively.

In (TM-TPDS-STP)PF$_6$(C$_6$H$_5$Cl), the DFT calculations at the UB3LYP/6-31G(d) level suggested that the HOMO-1 of Molecule A and B distributed to the (thiopyran-4-ylidene)-1,3-dithiole unit, and it is the same situation with the TM-PDS-STP salt as described above (Figure S2). Consequently, the overlap integrals were calculated by considering the HOMO-1 of the DFT calculation. The donors of the intermolecular interaction *p2* stacked with head-to-head manner and the (thiopyran-4-ylidene)-1,3-dithiole units interacted effectively with each other (Figures 11 and 12). Since the HOMO-1 distributed on the (thiopyran-4-ylidene)-1,3-dithiole unit of TM-TPDS-STP, the overlap integral *p2* (20.2×10^{-3}) is larger than those of *p1* and *p3* (15.7 and 12.6×10^{-3}), in which the donors stacked in a head-to-tail manner. The differences among the overlap integrals *p1*, *p2*, and *p3* led to the electronic tetramerization along the stacking direction. Since the thiopyran units of the interaction *c1* were adjacent to each other, the overlap integrals *c1* along the molecular long axis was relatively large. It

was found that (TM-TPDS-STP)PF$_6$(C$_6$H$_5$Cl) was a band insulator due to the electronic tetramerization and the D:A = 1:1 composition.

Figure 10. **(a)** Crystal structure of (TM-TPDS-STP)PF$_6$(C$_6$H$_5$Cl) viewed along the molecular short axis of TM-TPDS-STP. **(b)** Crystal structure of (TM-TPDS-STP)PF$_6$(C$_6$H$_5$Cl) viewed along the *b–a* axis.
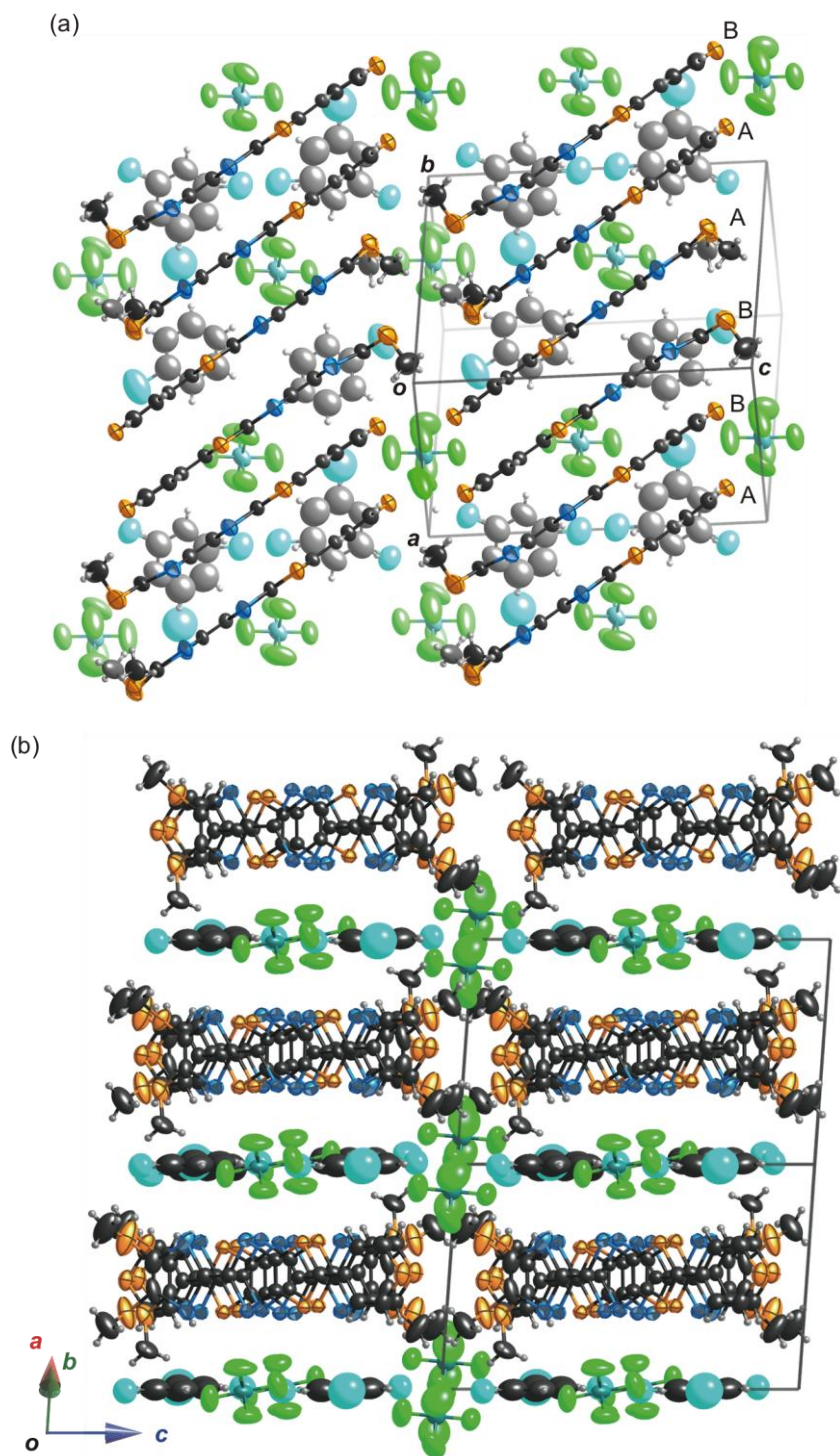
Figure 11. Molecular overlap modes for *p1*, *p2*, and *p3* of (TM-TPDS-STP)PF$_6$(C$_6$H$_5$Cl). The atoms and bonds of the depth molecules are faded out.

p1 (A-A, head-to-tail)   *p2* (A-B, head-to-head)
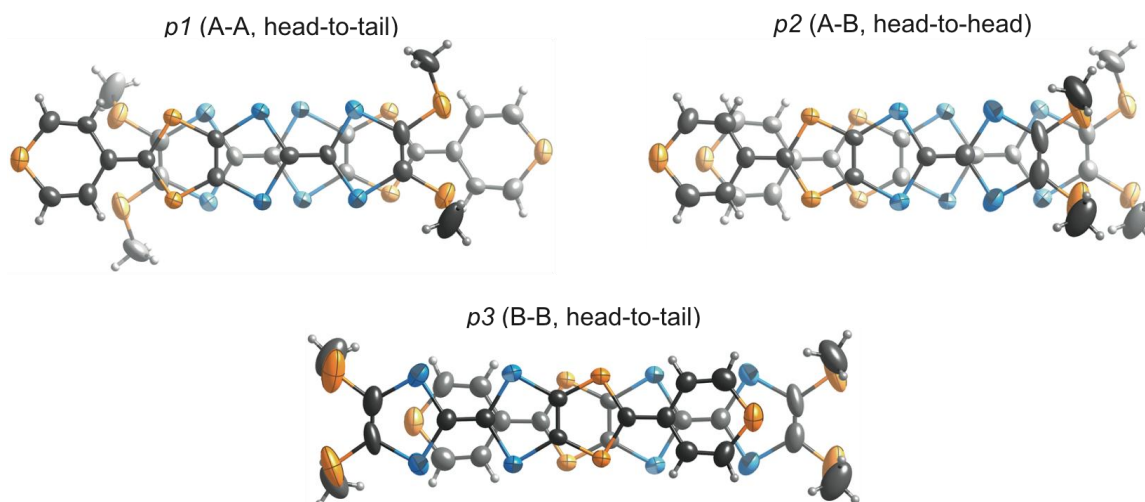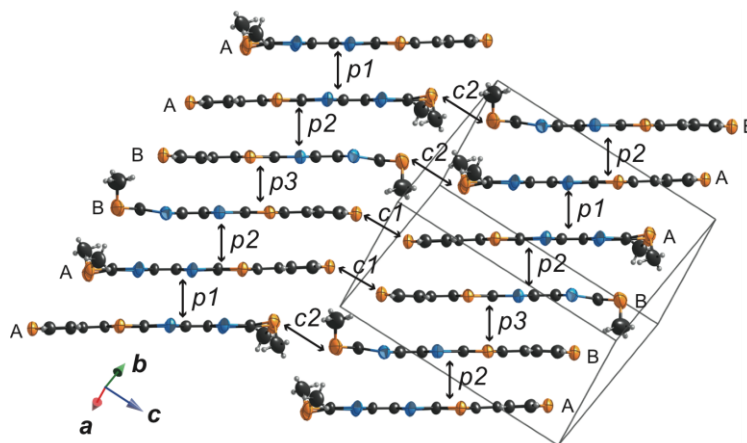
p3 (B-B, head-to-tail)

Figure 12. Donor sheet structure of (TM-TPDS-STP)PF$_6$(C$_6$H$_5$Cl) viewed along the molecular short axis. The calculated intermolecular overlaps between HOMO-1s ($\times 10^{-3}$) are *p1* = 15.7, *p2* = 20.2, *p3* = 12.6, *c1* = −2.0, and *c2* = 0.0022.

2.5. Electrical Properties of the Conducting Materials

Electrical properties of conducting materials based on **1** and **2** obtained so far are summarized in Table 2. The TCNQ complexes and the I$_3^-$ salts were prepared by mixing of the donors with TCNQ or Bu$_4$NI$_3$ in hot chlorobenzene. Compressed pellets of all the TCNQ complexes and the I$_3^-$ salts showed relatively high conductivity of $\sigma_{rt} = 10^{-1}$–10^1 S cm^{-1}. It is noted that electrical conductivity of the TCNQ complexes and the I$_3^-$ salt of TPDS-STP reached up to 20 S cm^{-1} at room temperature even the measurement of conductivity was carried out on a compressed pellet. Although resistivity of all the materials exhibited semiconductive temperature dependence, activation energies (E_a) of TCNQ complexes of **1b**, **2a**, **b** and I$_3^-$ salts of **1a** and **2a** were very small (0.017–0.040 eV). Empirically, a single crystal of these materials is expected to show metallic conducting behavior. On the other hand, room temperature conductivity of the PF$_6^-$ and AsF$_6^-$ salts of TM-PDS-STP and TM-TPDS-STP were not so high ($\sigma_{rt} = 10^{-3}$–10^{-2} S cm^{-1}). This result is consistent with those of X-ray structure analysis and

band calculation of the PF_6^- salts, that is, they are band insulators due to dimerized (tetramerized) stack of donors with fully ionized oxidation states.

Table 2. Electrical properties of conducting materials based on **1** and **2**.

Donor	Acceptor (Solvent)	D:A (:Solvent)	γ	σ_{rt} (S cm^{-1})[a]	E_a (eV)
PDS-STP **1a**	TCNQ	5:4	0.63	7.1×10^0	0.20
	I_3^-	5:4	0.8	1.6×10^0	0.040
TM-PDS-STP **1b**	TCNQ	1:1	0.72	3.9×10^{-1}	0.030
	I_3^-	5:4	0.8	3.2×10^{-1}	0.082
	PF_6^- (C_6H_5Cl)	1:1:0.5	1.0	1.8×10^{-3} [b]	0.22
TPDS-STP **2a**	TCNQ	5:4	0.73	1.8×10^1	0.033
	I_3^-	2:1	0.5	1.9×10^1	0.024
TM-TPDS-STP **2b**	TCNQ	3:2	0.45	9.1×10^0	0.017
	I_3^-	5:4	0.8	3.1×10^0	0.070
	PF_6^- (C_6H_5Cl)	1:1:1	1.0	3.7×10^{-2} [b]	0.16
	AsF_6^-			8.6×10^{-2} [b]	0.13

[a] Measured by four-probe method on a compressed pellet; [b] Measured on a single crystal.

3. Experimental Section

3.1. General

^{1}H NMR spectra were recorded on JEOL NM-SCM270 and JEOL NM-EX400 instrument. Spectra are reported (in δ) with referenced to Me_4Si. Mixture of CS_2 and C_6D_6 was used as a solvent. MS spectra were measured on Applied Biosystem MALDI TOFMS Voyager-DE^{TM} PRO. Melting points were determined with a Yanaco MP-J3. Cyclic voltammetry (CV) were recorded on ALS/chi 617B electrochemical analyzer. The CV cell consisted of Pt working electrode, Pt wire counter electrode, and an $Ag/AgNO_3$ reference electrode. The measurements were carried out in benzonitrile solution of sample with a concentrate 0.1 M $Bu_4N^+PF_6^-$ as a supporting electrolyte. All redox potentials were measured against Ag/Ag^+ and converted to vs. Fc/Fc^+. Electrical conductivity measurements were achieved using a Fuso-HECS 994 conductivity instrument in the temperature range 80–300 K. Electrical contacts were achieved with gold paste.

3.2. Synthesis

2-(1,3-diselenol-2-ylidene)-5-(tetrahydropyran-4-ylidene)-1,3-deselena-4,6-dithiapentalene (**6a**). Compound **3a** (250 mg, 0.502 mmol) and tetrahydro-4H-pyran-4-one (**4**) (151 mg, 1.51 mmol) was stirred in toluene (6 mL) and triethyl phosphite (6 mL) at 110 °C under argon for 2 h. After the reaction mixture was cooled to room temperature, *n*-hexane was added. The resultant precipitate was filtered, washed with *n*-hexane, and then column chromatographed on silica gel with carbon disulfide as an eluent. After evaporation of the solvent, compound **6a** (84 mg, 0.15 mmol) was obtained as brown powder in 30% yield. m.p. 223 °C (dec.); ^{1}H NMR (CS_2-C_6D_6 270 MHz): δ 2.05 (t, $J = 5.6$ Hz, 4H), 3.48 (t, $J = 5.6$ Hz, 4H), 6.98 (s, 2H); IR (KBr) v 2915, 1638, 1524, 1379, 1249, 1235, 1096, 1016 cm^{-1}; LDI-TOF-MS Calcd. for $C_{12}H_{10}OS_2Se_4$: 553.68 (M$^+$). Found: 551.67 with an isotropic pattern of these selenium atoms; Anal. Calcd. for $C_{12}H_{10}OS_2Se_4$: C, 26.20; H, 1.83. Found: C, 26.21; H, 1.85.

The other derivatives **6b**, **7a**, and **7b** were obtained by the similar procedure mentioned above.

2-[4,5-bis(methylthio)-1,3-diselenol-2-ylidene]-5-(tetrahydropyran-4-ylidene)-1,3-deselena-4,6-dithiapentalene (**6b**). Obtained in 36% yield (49 mg, 0.076 mmol) from **3b** (121 mg, 0.21 mmol) and tetrahydro-4H-pyran-4-one (**4**) (62 mg, 0.62 mmol) after column chromatography on silica gel with carbon disulfide. Dark brown powder; m.p. 229 °C (dec.); ^{1}H NMR (CS$_2$-C$_6$D$_6$ 270 MHz): δ 2.08 (t, J = 5.6 Hz, 4H), 2.35 (s, 6H), 3.51 (t, J = 5.6 Hz, 4H); IR (KBr) ν 2970, 2916, 2857, 1428, 1380, 1313, 1249, 1232, 1095, 1017 cm^{-1}; LDI-TOF-MS calcd. for C$_{14}$H$_{14}$OS$_2$Se$_4$: 643.66 (M$^+$). Found: 641.46 with an isotropic pattern of these selenium atoms; Anal. Calcd. for C$_{14}$H$_{14}$OS$_4$Se$_4$: C, 26.18; H, 2.20. Found: C, 26.15; H, 2.23.

2-(1,3-diselenol-2-ylidene)-5-(tetrahydrothiopyran-4-ylidene)-1,3-deselena-4,6-dithiapentalene (**7a**). Obtained in 39% yield (111 mg, 0.195 mmol) from **3a** (250 mg, 0.502 mmol) and 4-oxothiane (**5**) (234 mg, 2.02 mmol) after column chromatography on silica gel with carbon disulfide. Dark green powder; m.p. 217 °C (dec.); ^{1}H NMR (CS$_2$-C$_6$D$_6$ 270MHz) δ 2.31 (m, 4H), 2.47 (m, 4H), 6.96 (s, 2H); IR (KBr) ν 2907, 1528, 1423, 1270, 1171, 1000 cm^{-1}; LDI-TOF-MS Calcd. for C$_{12}$H$_{10}$S$_3$Se$_4$: 567.66 (M$^+$). Found: 569.18 with an isotropic pattern of these selenium atoms; Anal. Calcd. for C$_{12}$H$_{10}$S$_3$Se$_4$: C, 25.45; H, 1.78. Found: C, 25.39; H, 1.80.

2-[4,5-bis(methylthio)-1,3-diselenol-2-ylidene]-5-(tetrahydrothiopyran-4-ylidene)-1,3-deselena-4,6-dithiapentalene (**7b**). Obtained in 56% yield (94 mg, 0.14 mmol) from **3b** (150 mg, 0.254 mmol) and 4-oxothiane (**5**) (90 mg, 0.78 mmol) after column chromatography on silica gel with carbon disulfide. Dark green powder; m.p. 219 °C (dec.); ^{1}H NMR (CS$_2$-C$_6$D$_6$ 270 MHz) δ 2.36 (s, 6H), 2.36 (m, 4H), 2.51 (m, 4H); IR (KBr) ν 2913, 1638, 1421, 1271, 1171, 938 cm^{-1}; LDI-TOF-MS Calcd. for C$_{14}$H$_{14}$S$_5$Se$_4$: 657.64 (M$^+$). Found: 658.87 with an isotropic pattern of these selenium atoms; Anal. Calcd. for C$_{14}$H$_{14}$S$_5$Se$_4$: C, 25.54; H, 2.14. Found: C, 25.33; H, 2.09.

2-(1,3-diselenol-2-ylidene)-5-(pyran-4-ylidene)-1,3-diselena-4,6-dithiapentalene (**1a**). A solution of DDQ (51 mg, 0.22 mmol) in mixed xylene (24 mL) was added dropwise for 30 min to a stirred solution of **6a** (50 mg, 0.091 mmol) in mixed xylene (30 mL) at reflux under argon. After additional 30 min, the reaction mixture was cooled down to room temperature. Then, *n*-hexane was added, and the resultant precipitate was filtered. Purification by column chromatography on silica gel with carbon disulfide as an eluent afforded compound **1a** (28 mg, 0.051 mmol) was obtained as ocher powder in 55% yield. m.p. 204 °C; ^{1}H NMR (CS$_2$-C$_6$D$_6$ 270 MHz) δ 5.31 (d, J = 3.6 Hz, 2H), 6.30 (d, J = 3.6 Hz, 2H), 6.98 (s, 2H); IR (KBr) ν 1255, 1212, 1033, 901 cm^{-1}; LDI-TOF-MS Calcd. for C$_{12}$H$_6$OS$_2$Se$_4$: 547.65 (M$^+$). Found: 549.30 with an isotropic pattern of these selenium atoms; Anal. Calcd. for C$_{12}$H$_6$OS$_2$Se$_4$: C, 26.39; H, 1.11. Found: C, 26.17; H, 1.41.

The other derivatives **1b**, **2a**, and **2b** were obtained by the similar procedure mentioned above.

2-[4,5-bis(methylthio)-1,3-diselenol-2-ylidene]-5-(pyran-4-ylidene)-1,3-deselena-4,6-dithiapentalene (**1b**). Obtained in 75% yield (33 mg, 0.052 mmol) from **6b** (44 mg, 0.069 mmol) and DDQ (39 mg, 0.17 mmol) after column chromatography on silica gel with carbon disulfide. Ocher powder; m.p. 222 °C (dec.); ^{1}H NMR (CS$_2$-C$_6$D$_6$ 270 MHz) δ 2.32 (s, 6H), 5.3 (d, J = 3.6 Hz, 2H), 6.33 (d, J = 3.6 Hz, 2H); IR (KBr) ν 2913, 1663, 1429, 1254, 1034, 900 cm^{-1}; LDI-TOF-MS Calcd. for

$C_{14}H_{10}OS_4Se_4$: 639.63 (M^+). Found: 639.02 with an isotropic pattern of these selenium atoms; Anal. Calcd. for $C_{14}H_{10}OS_4Se_4$: C, 26.18; H, 2.20. Found: C, 25.95; H, 1.90.

2-(1,3-diselenol-2-ylidene)-5-(thiopyran-4-ylidene)-1,3-diselena-4,6-dithiapentalene (**2a**). Obtained in 51% yield (56 mg, 0.099 mmol) from **7a** (112 mg, 0.199 mmol) and DDQ (113 mg, 0.498 mmol) after column chromatography on silica gel with carbon disulfide. Ocher powder; m.p. 221 ℃ (dec.); ^{1}H NMR (CS_2-C_6D_6 270 MHz) δ 5.91 (s, 4H), 7.03 (s, 2H); IR (KBr) v 2920, 1637, 1542, 1509, 1421, 1038 cm^{-1}; LDI-TOF-MS Calcd. for $C_{12}H_6S_3Se_4$: 563.63 (M^+). Found: 563.25 with an isotropic pattern of these selenium atoms.

2-[4,5-bis(methylthio)-1,3-diselenol-2-ylidene]-5-(thiopyran-4-ylidene)-1,3-deselena-4,6-dithiapentalene (**2b**). Obtained in 86% yield (76 mg, 0.13 mmol) from **7b** (100 mg, 0.152 mmol) and DDQ (86 mg, 0.38 mmol) after column chromatography on silica gel with carbon disulfide. Ocher powder; m.p. 222 ℃ (dec.); ^{1}H NMR (CS_2-C_6D_6 270 MHz) δ 2.32 (s, 6H), 5.91(s, 4H); IR (KBr) v 2913, 1543, 1491, 1422, 1294, 1090 cm^{-1}; LDI-TOF-MS Calcd. for $C_{14}H_{10}S_5Se_4$: 655.61 (M^+). Found: 654.57 with an isotropic pattern of these selenium atoms; Anal. Calcd. for $C_{14}H_{10}S_5Se_4$: C, 25.70; H, 1.54. Found: C, 25.41; H, 1.55.

3.3. General Procedure for Preparation of TCNQ Complexes and I_3^- Salts

Hot solutions of donor molecule and TCNQ or tetra-*n*-butylammonium triiodide in chlorobenzene were mixed, and the resultant precipitate was collected by filtration. The TCNQ complex was washed with carbon disulfide and acetonitrile, and dried *in vacuo*. The I_3^- salts were washed with carbon disulfide and methanol, and dried *in vacuo*. The stoichiometry of TCNQ complexes and the I_3^- salts was determined by elemental analysis.

3.4. General Procedure for Preparation of Cation Radical Salts

Cation radical salts of **1b** and **2b** were prepared by electrochemical oxidation in chlorobenzene (5% ethanol, v/v, 18 mL) at a controlled current from 0.2 up to 1.0 μA in the presence of the corresponding tetra-*n*-butylammonium salts at 50 ℃ for 1–3 weeks. The crystals obtained were washed with ethanol and were air-dried at room temperature.

3.5. X-ray Crystallographic Analysis

The diffraction data were collected on a Rigaku Mercury70 diffractometer using graphite monochromated Mo-K_α radiation. (λ = 0.71070 Å). The structures were solved by the direct method (SIR97 [12]) and refined by full-matrix least squares on F^2 (SHELXL-97 [13]). Details concerning the crystal data collection and refinement parameters for TM-PDS-STP, (TM-PDS-STP)$PF_6(C_6H_5Cl)_{0.5}$, and (TM-TPDS-STP)$PF_6(C_6H_5Cl)$ are summarized in Table 3. CCDC-892512, CCDC-892513, and CCDC-892514 (for TM-PDS-STP, (TM-PDS-STP)$(PF_6)(C_6H_5Cl)_{0.5}$, and (TM-TPDS-STP)$PF_6(C_6H_5Cl)$) contain the supplementary crystallographic data for this paper. These data can be obtained free of charge from the Cambridge Crystallographic Data Centre via www.ccdc.cam.ac.uk/data_request/cif.

Table 3. Crystal data and structure refinement for TM-PDS-STP, (TM-PDS-STP)PF$_6$(C$_6$H$_5$Cl)$_{0.5}$, and (TM-TPDS-STP)PF$_6$(C$_6$H$_5$Cl).

Compound	TM-PDS-STP	(TM-PDS-STP)PF$_6$(C$_6$H$_5$Cl)$_{0.5}$	(TM-TPDS-STP)PF$_6$(C$_6$H$_5$Cl)
Formula	C$_{14}$H$_{10}$OS$_4$Se$_4$	C$_{16}$H$_{16}$F$_6$O$_2$PS$_4$Se$_4$	C$_{20}$H$_{15}$ClF$_6$PS$_5$Se$_4$
Formula weight	638.30	829.34	911.89
Crystal system	Monoclinic	Triclinic	Triclinic
Space group	$P2_1/n$	$P\bar{1}$	$P\bar{1}$
a (Å)	5.230(1)	7.917(3)	12.666(3)
b (Å)	11.006(2)	10.582(3)	14.299(4)
c (Å)	31.718(6)	15.979(5)	16.289(5)
α (°)	90	76.67(2)	85.39(2)
β (°)	93.903(6)	89.92(2)	88.219(19)
γ (°)	90	89.12(2)	79.79(2)
V (Å^3)	1821.4(6)	1302.5(7)	2894(1)
Z	4	2	2
λ (Å)	0.71070	0.71070	0.71070
D$_{calc}$ (mg m^{-3})	2.328	2.115	2.093
μ (mm^{-1})	8.514	6.072	5.631
Number of reflections collected	16677	13884	31475
Number of independent reflections	4129	5841	12916
Number of reflections with [$I > 2\sigma(I)$]	2787	2799	6484
Number of parameters refined	211	382	689
R	0.0601	0.0786	0.0749

3.6. Electronic Band Calculations

From the results of the crystal structure analysis, intermolecular overlap integrals were calculated by considering in the HOMO-1 of donor molecules obtained by the result of density functional theory (DFT) calculation at the UB3LYP/6-31G(d) level [14] using Gaussian 09 program package [15]. The electronic band dispersions and Fermi surfaces were calculated using the intermolecular transfer integrals under the tight-binding approximation [16].

4. Conclusions

Four kinds of new bis-fused donors composed of (thio)pyran-4-ylidene-1,3-dithiole and tetraselenafulvalene (**1a**, **2a**) and their bis(methylthio) derivatives tetraselenafulvalene (**1b**, **2b**) were successfully synthesized. The results of cyclic voltammetry indicated that a positive charge of **1**$^{+\bullet}$ and **2**$^{+\bullet}$ distributed mainly on the (thio)pyran-4-ylidene-1,3-dithiole moiety, probably due to more powerful donating ability of (thio)pyran-4-ylidene-1,3-dithiole than tetraselenafulvalene. Occurrence of such an intramolecular charge disproportionation in the radical cation salts (**1b**)PF$_6$(C$_6$H$_5$Cl)$_{0.5}$ and (**2b**)PF$_6$(C$_6$H$_5$Cl) was also suggested by the results of X-ray structure analysis and DFT calculation. The expected observation of "windmill" type structure was not observed, probably due to intramolecular charge disproportionation of the donors as well as 1:1 composition of the donor to anion. High conductivity found in the TCNQ complexes and the I$_3^-$ salts (σ_{rt} = 0.3–19 S cm^{-1} on a

compressed pellet) with very low activation energies (0.017–0.040 eV) brings high expectation that **1** and **2** are promising donor components for development of new molecular conductors. We are currently investigating synthesis of the analogues of **1** and **2**, in which selenium atoms are exchanged or added to the other positions of sulfurs, as well as preparation of molecular conductors of **1** and **2** with different anions.

Acknowledgments

References and Notes

1. For a recent review of TTP-based organic conductors, see Misaki, Y. Tetrathiapentalene-based organic conductors. *Sci. Technol. Adv. Mater.* **2009**, *10*, 024301:1–024301:22.
2. Misaki, Y.; Fujiwara, H.; Yamabe, T.; Mori, T.; Mori, H.; Tanaka, S. Structure and conducting properties of BDT-TTP salts. *Chem Lett.* **1994**, *23*, 1653–1656.
3. Misaki, Y.; Tanaka, K.; Taniguchi, M.; Yamabe, T.; Mori, T. Structures and electrical properties of (EO-TTP)$_2$AsF$_6$. *Chem. Lett.* **1999**, *28*, 1249–1250
4. Misaki, Y.; Fujiwara, H.; Maruyama, T.; Taniguchi, M.; Yamabe, T.; Mori, T.; Mori, H.; Tanaka, S. Novel oxygen containing π-electron donors for organic metals: 2-(1,3-dithiol-2-ylidene)-5-(pyran-4-ylidene)-1,3,4,6-tetrathiapentalenes. *Chem. Mater*. **1999**, *11*, 2360–2368.
5. Misaki, Y.; Fujiwara, H.; Yamabe, T. Novel bis-fused π-electron donors for organic metals: 2-(1,3-dithiol-2-ylidene)-5-(thiopyran-4-ylidene)-1,3,4,6-tetrathiapentalene. *J. Org. Chem.* **1996**, *61*, 3650–3656.
6. Misaki, Y.; Kaibuki, T.; Taniguchi, M.; Tanaka, K.; Kawamoto, T.; Mori, T.; Nakamura, T. A Novel organic conductor with three-dimensional donor array: (TM-TPDS)$_2$AsF$_6$. *Chem. Lett*. **2000**, *29*, 1274–1275.
7. Takahashi, K.; Nakayashiki, T.; Taniguchi, M.; Misaki, Y.; Tanaka, K. A novel organic conductor with two-dimensional molecular array by the "edge-to-edge" donor interaction. *Chem. Lett.* **2001**, *30*, 162–163.
8. Ishizu, K.; Watanabe, M.; Tanahashi, T.; Misaki, Y.; Ashizawa, M.; Mori, T. Synthesis and properties of new TTP donors composed of TTF and TSF moieties. *J. Phys. Confer. Ser.* **2008**, *132*, 012021:1–012021:5.
9. Ashizawa, M.; Ishizu, K.; Watanabe, M.; Tanahashi, T.; Shirahata, T.; Kawamoto, T.; Mori, T.; Misaki, Y. Novel bis-fused π-electron donor composed of tetrathiafulvalene and tetraselenafulvalene. *Chem. Lett.* **2010**, *39*, 1093–1095.
10. Bondi, A. van der Waals volumes and radii. *J. Phys. Chem.* **1964**, *68*, 441–451.

11. Anzai, H.; Delrieu, J.M.; Takasaki, S.; Nakatsuji, S.; Yamada, J. Crystal growth of organic charge-transfer complexes by electrocrystallization with controlled applied current. *J. Cryst. Growth* **1995**, *154*, 145–150.

12. Altomare, A.; Burla, M.; Camalli, M.; Cascarano, G.; Giacovazzo, C.; Guagliardi, A.; Moliterni, A.; Polidori, G.; Spagna, R. SIR97: a new tool for crystal structure determination and refinement. *J. Appl. Cryst.* **1999**, *32*, 115–119.

13. Sheldrick, G.M. *SHELX-97, Program for the Refinement of Crystal Structures*; University of Gottingen: Gottingen, Germany, 1996.

14. Hehre, W.J.; Ditchfield, R.; Pople, J.A. Self—Consistent molecular orbital methods. XII. Further extensions of Gaussian—Type basis sets for use in molecular orbital studies of organic molecules. *J. Chem. Phys.* **1972**, *56*, 2257–2261.

15. Frisch, M.J.; Trucks, G.W.; Schlegel, H.B.; Scuseria, G.E.; Robb, M.A.; Cheeseman, J.R.; Scalmani, G.; Barone, V.; Mennucci, B.; Petersson, G.A.; *et al. Gaussian 09*, Revision C.01; Gaussian, Inc.: Wallingford, CT, USA, 2011.

16. Mori, T.; Kobayashi, A.; Sasaki, Y.; Kobayashi, H.; Saito, G.; Inokuchi, H. The intermolecular interaction of tetrathiafulvalene and bis(ethylenedithio)tetrathiafulvalene in organic metals. Calculation of orbital overlaps and models of energy-band structures. *Bull. Chem. Soc. Jpn.* **1984**, *57*, 627–633.